ISSN: 2319-5967
ISO 9001:2008 Certified
International Journal of Engineering Science and Innovative Technology (IJESIT)
Volume 2, Issue 5, September 2013

Image and Video Quality Assessment with BLIINDS-II Algorithm using NSS Approach in DCT domain

M. Santhoshi, S. Aruna Kumari, S. Srikanth Reddy, A. Vijay Kumar

Abstract*— we develop an efficient BLIINDS-II algorithm using NSS approach in DCT domain for image and video quality assessment with no reference image. The approach relies on a simple Bayesian inference model to predict image and video quality score, after a set of features is extracted from an image. These features are extracted from a generalized NSS based model of local DCT coefficients. Generalized Gaussian density model parameters are used to form these features. BLIINDS-II (Blind Image Integrity notator using DCT Statistics-II) adopts a simple probabilistic model for score prediction. Given the extracted features from a test image/video, the quality score that maximizes the probability of the empirically determined inference model is chosen as the predicted quality score of that image/video. When tested on the LIVE IQA database, BLIINDS-II correlates highly with the human judgments of quality.

***Index Terms*— Bayesian inference model, Image quality assessment (IQA), Natural scene statistics, Video quality assessment (VQA).**

I. INTRODUCTION

Digital video data, stored in video databases and distributed through communication networks, is subject to various kinds of distortions during acquisition, compression, processing, transmission, and reproduction. For example, lossy video compression techniques, which are almost always used to reduce the bandwidth needed to store or transmit video data, may degrade the quality during the quantization process. It is therefore imperative for a video service system to be able to realize and quantify the video quality degradations [8] that occur in the system, so that it can maintain, control and possibly enhance the quality of the video data. An effective image and video quality metric is crucial for this purpose.

The most reliable way of assessing the quality of an image or video is subjective evaluation, because human beings are the ultimate receivers in most applications. The mean opinion score (MOS), which is a subjective quality measurement obtained from a number of human observers, has been regarded for many years as the most reliable form of quality measurement. However, the MOS method is too inconvenient, slow and expensive for most applications which lead to the objective image and video quality assessment.

The goal of objective image and video quality assessment research is to design quality metrics that can predict perceived image and video quality automatically.

Objective image and video quality metrics can be classified according to the availability of the original image and video signal, which is considered to be distortion-free or perfect quality, and may be used as a reference to compare a distorted image or video signal against. Most of the proposed objective quality metrics in the literature assume that the undistorted reference signal is fully available. Although “image and video quality” is frequently used for historical reasons, the more precise term for this type of metric would be image and video similarity or fidelity measurement, or full-reference (FR) image and video quality assessment.

It is worth noting that in many practical video service applications, the reference images or video sequences are often not accessible. So, certain features are extracted from the original signal and transmitted to the quality assessment system as side information to help evaluate the quality of the distorted image or video. This is referred to as reduced-reference (RR) image and video quality assessment.

There exists an image and video quality assessment method, in which the original image or video signal is not fully available i.e., It is highly desirable to develop measurement approaches that can evaluate image and video quality blindly. Blind or no-reference (NR) image and video quality assessment turns out to be a very difficult task, although human observers usually can effectively and reliably assess the quality of distorted image or video without using any reference

ISSN: 2319-5967
ISO 9001:2008 Certified
International Journal of Engineering Science and Innovative Technology (IJESIT)
Volume 2, Issue 5, September 2013

We introduce the recent effort by the video quality experts group (VQEG) [1], which aims to provide industrial standards for video quality assessment. The philosophy of doing NR or RR quality assessment will continue to be that of blind distortion measurement with respect to features that best separate the undistorted signals from the distortion. The success of statistical models for natural scenes that are more suited to certain distortion types and applications will drive the success of NR and RR metrics. A combination of natural scene models with HVS models may also prove beneficial for NR and RR quality assessment.

The recent Motion-based Video Integrity Evaluation (MOVIE) index for video quality assessment utilizes a general, spatio-spectrally localized multi-scale framework for evaluating dynamic video fidelity that integrates both spatial and temporal (and spatio-temporal) aspects of distortion assessment. Video quality is evaluated not only in space and time, but also in space-time, by evaluating motion quality along computed motion trajectories. The MOVIE index delivers quality scores that correlate quite closely with human subjective judgment, using the Video Quality Expert Group (VQEG) LIVE Video Quality Database. One obvious way to implement video quality metrics is to apply a still image quality assessment metric on a frame-by-frame basis. The recent NR-IQA algorithms generally follow one of three trends: (i) Distortion-specific approaches (ii) Training based approaches (iii) Natural scene statistics (NSS) approaches.

A. NR-IQA metrics are

i). DIIVINE (Distortion Identification based Image Verify & Integrity Evaluation)

DIIVINE index is a combination of the second & third approaches and utilizes a 2-stage framework for blind IQA that first identifies the distortion afflicting the image and then performs distortion-specific quality assessment. [2] DIIVINE uses a support vector machine (SVM) to classify an image into a distortion class and support vector regression to predict quality scores. A large number of features are used for classification and for quality score prediction (88 features) to achieve high performance against human quality judgments.

ii). BLIINDS-I (Blind Image Integrity notator using DCT Statistics-I):

The BLIINDS index which is a no-reference approach to predict image quality assessment does not assume a specific type of distortion of the image and completely based on observing the statistics of local discrete cosine transform coefficients.

We propose an alternate approach that relies on a statistical model of local discrete cosine transform (DCT) coefficients which we dub blind image integrity notator using DCT statistics (BLIINDS-II). The new BLIINDS-II index advances the ideas embodied in an earlier prototype (BLIINDS-I) [3], which uses no statistical modeling and a different set of sample DCT statistics.

It uses a simple Bayesian approach to predict quality scores after a set of features is extracted from an image. For feature extraction, a generalized NSS based model of local DCT coefficients is estimated. The model parameters are used to design features suitable for perceptual image quality score prediction. The NSS features are used by the Bayesian probabilistic inference model to infer visual quality.

BLIINDS-II is non-distortion-specific, while most NR-IQA algorithms quantify a specific type of distortion; the features we use are derived independently of the type of image distortion and are effective across multiple distortion types.

II. IMPLEMENTATION OF THE METHOD

Un-distorted images captured by imaging devices that sense radiation from the visible spectrum as Natural scenes, and statistical models built for undistorted natural scenes as NSS models. The model-based NSS-IQA approach developed here is a process of feature extraction from the image, followed by statistical modeling of the extracted features.

Our approach relies on the IQA algorithm learning, how the NSS model parameters vary across different perceptual levels of image distortion. The algorithm is trained using features derived directly from a generalized parametric statistical model of natural image DCT coefficients against various perceptual levels of image distortion. The learning model is then used to predict perceptual image quality scores.

NSS models reflect statistical properties of the world that drive perceptual functions of the HVS. Characteristics that can be incorporated into NSS models include: 1) visual sensitivity to structural information [4], [5]; 2) perceptual masking [6] 3) visual sensitivity to directional information.

ISSN: 2319-5967
ISO 9001:2008 Certified
International Journal of Engineering Science and Innovative Technology (IJESIT)
Volume 2, Issue 5, September 2013

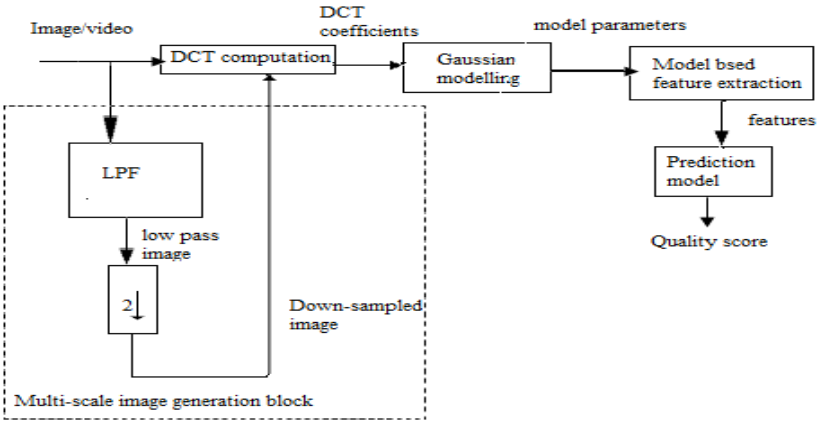

Fig 1.Framework of BLIINDS-II Algorithm

A. DCT Feature Domain and Computation

The first stage of the pipeline deals about feature extraction in the DCT domain is the observation that the statistics of DCT coefficients change with the degree and type of image distortion. Another advantage is computational convenience: optimized DCT-specific platforms, and fast algorithms for DCT computation, can ease computation. Many image and video compression algorithms are based on block-based DCT transforms (JPEG, MPEG2, H263, and H264 that relies on a variation of the DCT).

An image entering the IQA "pipeline" is first subjected to local 2-D DCT coefficient computation. This stage of the pipeline consists of partitioning the image into equally sized n x n blocks, henceforth referred to as local image patches, then computing a local 2-D DCT on each of the blocks. The coefficient extraction is performed locally in the spatial domain in accordance with the HVS's property of local spatial visual processing (i.e., in accordance with the fact that the HVS processes the visual space locally). This DCT decomposition is accomplished across spatial scales.

Table I. Matrix of DCT Coefficients

DC	C_{12}	C_{13}	C_{14}	C_{15}
C_{21}	C_{22}	C_{23}	C_{24}	C_{25}
C_{31}	C_{32}	C_{33}	C_{34}	C_{35}
C_{41}	C_{42}	C_{43}	C_{44}	C_{45}
C_{51}	C_{52}	C_{53}	C_{54}	C_{55}

B. Gaussian Modeling

The second stage of the pipeline applies a generalized Gaussian density model to each block of DCT coefficients, as well as for specific partitions within each DCT block. In order to capture directional information from the local image patches, the DCT block is partitioned directionally as into three oriented sub-regions.

Table II. Orientation-I of DCT coefficients

DC	C_{12}	C_{13}	C_{14}	C_{15}
C_{21}	C_{22}	C_{23}	C_{24}	C_{25}
C_{31}	C_{32}	C_{33}	C_{34}	C_{35}
C_{41}	C_{42}	C_{43}	C_{44}	C_{45}
C_{51}	C_{52}	C_{53}	C_{54}	C_{55}

ISSN: 2319-5967
ISO 9001:2008 Certified
International Journal of Engineering Science and Innovative Technology (IJESIT)
Volume 2, Issue 5, September 2013

Table III. Orientation-II of DCT coefficients

DC	C_{12}	C_{13}	C_{14}	C_{15}
C_{21}	C_{22}	C_{23}	C_{24}	C_{25}
C_{31}	C_{32}	C_{33}	C_{34}	C_{35}
C_{41}	C_{42}	C_{43}	C_{44}	C_{45}
C_{51}	C_{52}	C_{53}	C_{54}	C_{55}

The partition reflects three radial frequency sub-bands in the DCT block. The upper, middle, and lower partitions correspond to the low-frequency, mid-frequency, and high-frequency DCT sub-bands, respectively.

A generalized Gaussian fit is obtained for each of the radial DCT coefficient sub-regions as well. The introduction of distortions to the images changes the distribution of the coefficients. Gaussian family of distributions encompasses a wide range of observed behavior of distorted DCT coefficients. The uni-variate generalized Gaussian density is given by,

$$f(x \mid \alpha, \beta, \gamma) = \alpha e^{-(\beta|X-\mu|)^{\gamma}} \quad (1)$$

where, μ is Mean, α is Normalizing parameter, β is Scale parameter, γ is Shape parameter and are given by,

$$\alpha = \frac{\beta\gamma}{2\Gamma(1/\gamma)} \quad (2)$$

$$\beta = \frac{1}{\sigma}\sqrt{\frac{\Gamma(3/\gamma)}{\Gamma(1/\gamma)}} \quad (3)$$

where, σ is the standard deviation, and Γ denotes the gamma function given by,

$$\Gamma(z) = \int_0^{\infty} t^{z-1} e^{-t}\, dt \quad (4)$$

C. Feature extraction

The third step of the pipeline computes functions of the derived generalized Gaussian model parameters. These are the features used to predict image quality scores. In the following sections, we define and analyze each model-based feature, demonstrate how it changes with visual quality, and examine how well it correlates with human subjective judgments of quality.

D. Prediction model

The fourth and final stage of the pipeline is a simple Bayesian model that predicts a quality score for the image. The Bayesian approach maximizes the probability that the image has a certain quality score given the model-based features extracted from the image.

III. MODEL BASED FEATURE EXTRACTION

The parameters of the Gaussian modeling are then utilized to extract features for perceptual quality score prediction. The four extracted features are:

A. Generalized Gaussian Model Shape Parameter

From the Generalized Gaussian model of the non-*DC* DCT coefficients from *n x n* blocks, the shape parameter is derived. However, the *DC* coefficient does not convey structural information about the block, including it neither increases nor decreases performance.

The shape parameter γ is a model-based feature that is computed over all blocks in the image. The shape parameter quality feature is pooled in two ways i.e., 10^{th} percentile (average of local block scores across the image), 100^{th} percentile (the average (ordinary sample mean) of the local scores across the image), which shows improved correlations with subjective perception of quality. Therefore both 10^{th} and 100^{th} percentile pooling helps to inform the predictor whether the distortions are uniformly annoying over space or exhibit isolated perceptually severe distortions.

B. Coefficient of Frequency Variation

Let X is a random variable representing the histogram med DCT coefficients. The coefficient of frequency variation feature is given by,

$$\zeta = \frac{\upsilon_{|x|}}{\mu_{|x|}} \quad (5)$$

It is equivalent to,

ISSN: 2319-5967
ISO 9001:2008 Certified
International Journal of Engineering Science and Innovative Technology (IJESIT)
Volume 2, Issue 5, September 2013

$$\zeta = \sqrt{\frac{\Gamma(1/\gamma)\Gamma(3/\gamma)}{\Gamma^2(2/\gamma)} - 1} \quad (6)$$

Where, $\sigma_{|X|}$ and $\mu_{|X|}$ are the standard deviation and mean of the DCT coefficient magnitudes $|X|$, respectively. If X has probability density function (1) and $\mu_X = 0$, then

$$\mu_{|X|} = \int_{-\infty}^{+\infty} |X| \alpha e^{-(\beta|x|)^{\gamma}} dx = \frac{2\alpha}{\beta^2 \gamma} \Gamma\left(\frac{2}{\gamma}\right) \quad (7)$$

Where, α and β are given by (2) and (3), respectively. Substituting for α and β yields

$$\frac{\Gamma(1/\gamma)\Gamma(3/\gamma)}{\Gamma^2(2/\gamma)} = \frac{\sigma^2}{\mu^2_{|x|}} \quad (8)$$

Further,

$$\sigma^2_{|X|} = \sigma^2_X - \mu^2_{|X|} \quad (9)$$

$$\zeta = \frac{\upsilon_{|x|}}{\mu_{|x|}} = \sqrt{\frac{\Gamma(1/\gamma)\Gamma(3/\gamma)}{\Gamma^2(2/\gamma)} - 1} \quad (10)$$

And σX is the standard deviation of X.

The feature ζ is computed for all blocks in the image. The feature is pooled by averaging over the highest 10th percentile and overall (100th percentile) of the local block scores across the image. As before, both pooling results (10% and 100%) are supplied to the predictor, since the difference between these is a compact but rich form of information regarding the distribution of severe scores.

C. Energy Sub-band Ratio Measure

Image distortions often modify the local spectral signatures of an image in ways that make them dissimilar to the spectral signatures of pristine images. To determine the local spectral signatures, a local DCT energy sub-band ratio has to measure.

Consider the 5×5 matrix arrangement of DCT coefficients. Moving from the top-left corner of the matrix toward the bottom-right corner, the DCT coefficients represent increasingly higher radial spatial frequencies.

The three frequency bands depicted by different levels of shading are represented in Orientation-II of DCT coefficients. The average energy in frequency band n is defined as the model variance σ_n^2 corresponding to band n and is given by,

$$E_n^2 = \sigma_n^2 \quad (11)$$

This is found by fitting the DCT data histogram in each of the three spatial frequency bands to the generalized Gaussian model (1), and then using the σ_n^2 value from the fit. The ratio of the difference between the average energy in frequency band n and the average energy up to frequency band n, as well as the sum of these two quantities is then computed and is given by,

$$R_n = \frac{\left|E_n - \frac{1}{n-1}\sum_{j<n} E_j\right|}{E_n + \frac{1}{n-1}\sum_{j<n} E_j} \quad (12)$$

This feature measures the relative distribution of energies in lower and higher bands, which can be affected by distortions. The mean of R2 and R3 is computed and this feature is computed for all blocks in the image. As before, the feature is pooled by computing the highest 10th percentile average and the 100th percentile average (ordinary mean) of the local block scores across the entire image.

D. Orientation Model-Based Feature

Image distortions often modify local orientation energy in an unnatural manner. The HVS, which is highly sensitive to local orientation energy, is likely to respond to these changes. To capture directional information in the image that may correlate with changes in human subjective impressions of quality, the block DCT coefficients along three orientations has to model as shown in either orientation-I or II**.** The three differently shaded areas represent the DCT coefficients along three orientation bands. A generalized Gaussian model is fitted to the coefficients within each shaded region in the block, and ζ is obtained from the model histogram fits for each orientation. The variance of ζ is computed along each of the three orientations. The variance of ζ across the three orientations from all the blocks in the image is then pooled (highest 10th percentile and 100th percentile averages) to obtain two numbers per image. These pooled features correlates with subjective DMOS.

ISSN: 2319-5967
ISO 9001:2008 Certified
International Journal of Engineering Science and Innovative Technology (IJESIT)
Volume 2, Issue 5, September 2013

IV. MULTI-SCALE FEATURE EXTRACTION

The implementation of BLIINDS-II concept over multiple scales is a simple way, in which the NSS-based DCT features are extracted from 5×5, overlapping blocks in the image. The feature extraction is repeated after low-pass filtering the image and sub-sampling it by a factor of 2 as shown in below fig 2.

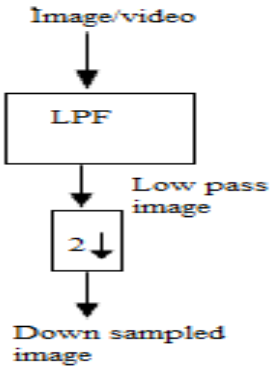

Fig 2. Multi scale image generation

Prior to down-sampling, the image is filtered by a rotationally symmetric discrete 3×3 Gaussian filter kernel (see table IV).

Table IV. Gaussian kernel

0.0113	0.0838	0.0113
0.0838	0.6193	0.0838
0.0113	0.0838	0.0113

At each scale, the overlap between neighboring blocks is two pixels. This defines a multi-scale feature extraction approach. Multi-scale feature extraction and processing generally improves performance when dealing with changes in the image resolution, distance from the image display to the observer, or variations in the acuity of the observer's visual system. In BLIINDS-II, feature extraction over multiple scales makes it possible to capture variations in the degree of distortion over scales.

V. PREDICTION MODEL

We have found that a simple probabilistic predictive model is adequate for training the features used in BLIINDS-II. The prediction model is the only element of BLIINDS-II that carries over from BLIINDS-I. The efficacy of this simple predictor demonstrates the effectiveness of the NSS-based features used by BLIINDS-II to predict image quality.

Let $Xi = [x_1, x_2, ..., x_m]$ be the vector of features extracted from the image, where i is the index of the image being assessed, and m be the number of pooled features that are extracted. Additionally, let $DMOS_i$ be the subjective DMOS associated with the image i. We model the distribution of the pair $(Xi, DMOS_i)$.

The probabilistic model is trained on a subset of the LIVE IQA database, which includes DMOS scores, to determine the parameters of the probabilistic model by distribution fitting. The multivariate GGD model is used to model the data and is given by,

$$f(x|\alpha, \beta, \gamma) = \alpha e^{-(\beta(x-\mu)^T\sum^{-1}(x-\mu))^\gamma} \quad (13)$$

Parameter estimation only requires the mean and covariance of the empirical data from the test set. The probabilistic model $P(X, DMOS)$ is applied by fitting (13) to the empirical data of the training set. Specifically, once the quantity $(x-\mu)^T\sum^{-1}(x-\mu))^\gamma$ is estimated from the sample data, parameter estimation of the GGD model in (13) is performed using the fast method.

The distribution fitting ($P(X, DMOS)$) on the training data is only a fast intermediate step toward DMOS prediction. The end goal is not to fit the sample data of the training set as accurately as possible to the prediction model. Instead, the aim is to achieve high correlations between predicted and subjective DMOS using this prediction model.

The probabilistic model is then used to perform prediction by maximizing the quantity $P(DMOS_i | X_i)$. This is equivalent to maximizing the joint distribution $P(X, DMOS)$ of X and DMOS since $P(X, DMOS) = P(DMOS|X) p(X)$.

ISSN: 2319-5967
ISO 9001:2008 Certified
International Journal of Engineering Science and Innovative Technology (IJESIT)
Volume 2, Issue 5, September 2013

VI. RESULTS

BLIINDS-II was rigorously tested on the LIVE IQA database [7], in which each image is impaired by many levels of five distortion types: JPEG2000, JPEG, white noise, Gaussian blur, and fast-fading channel distortions.
These eight pooled features are: The lowest 10^{th} percentile of the shape parameter γ, mean of the shape parameter γ, highest 10^{th} percentile of the coefficient of frequency variation ζ, mean (100^{th} percentile) of the coefficient of frequency variation ζ, highest 10^{th} percentile of the energy sub-band ratio measure R_n, mean of the energy sub-band ratio measure, highest 10^{th} percentile of the orientation feature (which is the variance of ζ across the three orientations) and the mean of the orientation feature. We illustrate all pooled features of 5 different images (see Table V).

Table V. Overall features of different image distortion types

	γ		ζ		Sub-band feature		Orientation feature	
LIVE subset	10%	100%	10%	100%	10%	100%	10%	100%
jpg	2.0453	3.5575	0.5829	1.9114	0.8390	0.9904	0.3274	1.5381
jpg2000	1.7370	3.2346	0.5985	1.3404	0.7790	0.9830	0.1887	0.8247
wn	1.5500	2.7379	0.6877	1.5183	0.7362	0.9702	0.1265	0.4938
gblur	2.1713	3.2872	0.4112	0.6622	0.8942	0.9875	0.1444	0.5098
Fast-fading	2.0786	3.3786	0.4557	0.8380	0.8421	0.9866	0.1753	0.6057

Also the model based-features were extracted over three scales. The total number of features per scale is 8 (4 features, 2 pooling methods/feature). Quality score prediction results for features extracted at one scale only (8 features), over two scales (16 features, 8 features per scale), and over three scales (24 features, 8 per scale). The 24 pooled features of jpg images have been obtained (see Table VI and VII).

Table VI 8-pooled features for multi-scale images

LIVE subset		BLIINDS-II	BLIINDS-II (2-Scale)	BLIINDS-II (4-Scale)
γ	10%	1.7060	1.4858	1.4741
	100%	2.9155	2.4167	2.3603
ζ	10%	0.5760	0.7972	0.6941
	100%	1.0959	0.3234	0.3143
Sub-band feature	10%	0.7543	0.7174	0.7554
	100%	0.9796	0.9636	0.9555
Orientation feature	10%	0.1220	0.1377	0.1645
	100%	0.4742	0.5364	0.6107

ISSN: 2319-5967
ISO 9001:2008 Certified
International Journal of Engineering Science and Innovative Technology (IJESIT)
Volume 2, Issue 5, September 2013

Table VII. 8-pooled features for multi-scale images

LIVE subset		BLIINDS-II	BLIINDS-II (2-SCALE)	BLIINDS-II (4-SCALE)
γ	10%	1.3780	1.4811	1.6617
	100%	2.6922	2.9568	3.0511
ζ	10%	0.9175	0.8135	0.7294
	100%	2.2690	0.3143	0.2766
Sub-band feature	10%	0.6644	0.7141	0.7399
	100%	0.9505	0.9565	0.9653
Orientation feature	10%	0.1345	0.1929	0.2515
	100%	0.6273	0.9190	0.9399

Scatter plots (for each of the distortion sets as well as for the entire LIVE IQA Database) of the predicted DMOS using BLIINDS-II versus subjective DMOS on the test sets are shown in below fig 3-7. The video quality assessment is also obtained for the given video as 60.32% predicted score and as shown in fig 8.

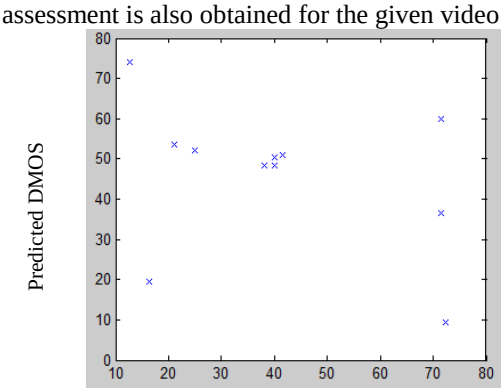

Fig 3. Predicted versus subjective DMOS on the JPEG2000 database

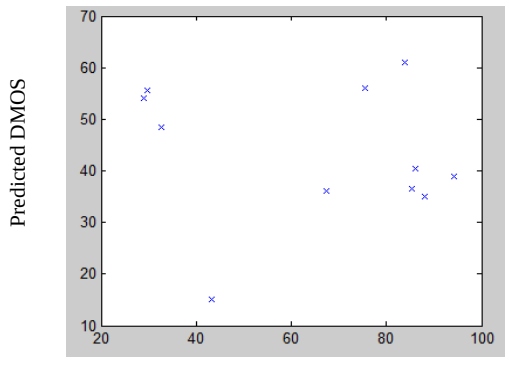

Fig 4. Predicted versus subjective DMOS on the JPEG database

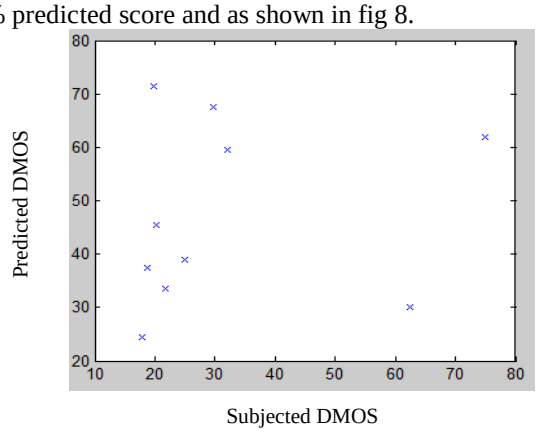

Fig 5. Predicted versus subjective DMOS on the white noise

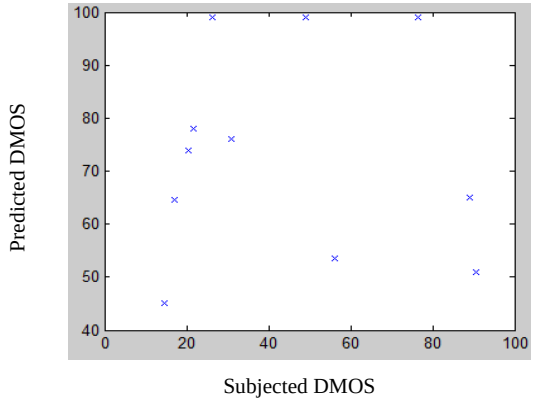

Fig 6. Predicted versus subjective DMOS on the Gaussian blur database

ISSN: 2319-5967
ISO 9001:2008 Certified
International Journal of Engineering Science and Innovative Technology (IJESIT)
Volume 2, Issue 5, September 2013

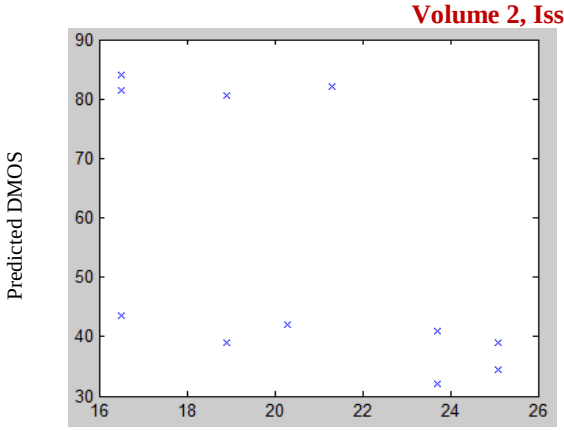

Fig 7. Predicted versus subjective DMOS on the fast-fading database

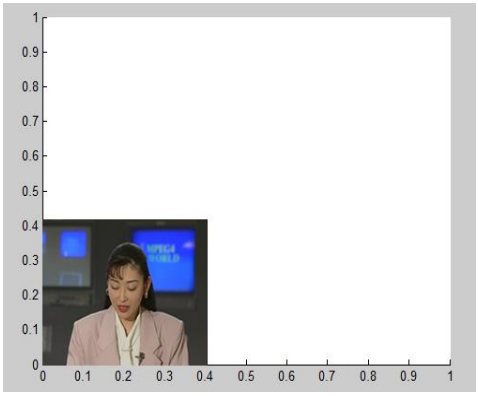

Fig 8. Conference.avi with predicted score 60.32%

VII. CONCLUSION

Therefore**,** a natural scene statistic model-based approach to the no-reference/blind Image and video QA problem has been described. The new NR-Image and video QA model uses a small number of computationally convenient DCT-domain features. The method correlates highly with human visual judgments of quality and it adopts a much simpler representation. It uses a lower dimensional feature space and a simpler single-stage (Bayesian prediction based) framework operating in a more sparsely sampled DCT domain. We envision that the BLIINDS-II approach may also be extendable to scenarios involving DCT-like transforms such as the H.264 integer transforms.

REFERENCES

[1] VQEG: The Video Quality Experts Group, http://www.vqeg.org.

[2] A. K. Moorthy and A. C. Bovik, "Blind image quality Assessment: From natural scene statistics to perceptual quality, IEEE Trans.Image Process., vol. 20, no. 12, pp.3350–3364, Dec. 2011.

[3] M. A. Saad, A. C. Bovik, andC. Charier, "A DCT statistics- based blind image quality index," IEEE Signal Process. Lett. vol. 17, no. 6, pp. 583–586, Jun. 2010.

[4] Z. Wang, A. C. Bovik , H. R. Sheikh and E. P. Simoncelli, "Image quality assessment: From error visibility to structural similarity," IEEE Trans. Image Process., vol. 13, no. 4, pp. 600–612, Apr. 2004.

[5] Z. Wang, E. P. Simoncelli, and A. C. Bovik,"Multiscale Structural Similarity image quality assessment," in Proc. 37th Asilomar Conf. Signals Syst. Comput., Nov. 2003, pp. 1398–1402.

[6] Q.Li and Z. Wang, "Reduced - reference image quality assessment using divisive - normalization -based image representation,"IEEE J. Sel. Topics Signal Process. vol. 3, no. 2, pp. 202–211, Apr. 2009.

[7] H. R. Sheikh, Z. Wang, L. Cormack, and A. C Bovik. LIVE Image Quality Assessment Database Release 2 [Online]. Available: http://live.ece.utexas.edu/research/quality.

[8] M. H. Pinson and S. Wolf, "A new standardized method for objectively measuring video quality," IEEE Trans. Broadcast, vol. 10, no. 3, pp.312–322, Sep. 2004.

ISSN: 2319-5967
ISO 9001:2008 Certified
International Journal of Engineering Science and Innovative Technology (IJESIT)
Volume 2, Issue 5, September 2013

AUTHOR BIOGRAPHY

M. Santhoshi received B. Tech degree in Electronics and Communication Engineering from JNTU affiliated college in 2009 and Pursuing M. Tech in Systems and Signal Processing from JNTU affiliated college.

S. Aruna Kumari received B. Tech degree in Electronics and Communication Engineering from JNTU affiliated college in 2006 and M. Tech in Communication Systems from JNTU affiliated college. Presented International conference on "Content based Image Retrieval". She is working as an Asst. Prof. in JNTU affiliated college, Hyderabad, INDIA.

S. Srikanth Reddy received B. Tech degree in Automobile Engineering from JNTU affiliated college in 2009 and awarded with Gold medal for Academic topper.

A. Vijay Kumar received B. Tech degree in Electronics and Communication Engineering from JNTU affiliated college in 2009 and Pursuing M. Tech in VLSI and Embedded Systems from JNTU affiliated college.